Revista de metalurgia

Application of Kramers-Kronig relationships for titanium impedance data validation in a Ringer's solution(•)

D.M. Bastidas*, E. Cano**, J.A. López-Caballero**, J.L. Polo*** and J.M. Bastidas**

Abstract This paper studies the applicability of Kramers-Kronig (KK) relationships to assess the validity of real and imaginary impedance measurements for titanium in a Ringer's solution using the electrochemical impedance spectroscopy (EIS) method. Nyquist and Bode plots showed a capacitive behaviour with a high impedance modulus including two time constants. Two procedures were employed in the implementation of the KK integral relationships based on an equivalent circuit which satisfies KK relationships and an ohmic resistance shunted to the measured EIS data. The titanium's EIS data satisfied the KK relationships.

Keywords Titanium. Ringer's solution. Kramers-Kronig relationships. Electrochemical impedance spectroscopy data.

Aplicación de las relaciones de Kramers-Kronig al estudio de la validez de las medidas de impedancia del titanio en la solución de Ringer

Resumen Este artículo estudia la aplicabilidad de las relaciones de Kramers-Kronig (KK) al estudio de la validez de las medidas de impedancia (EIS), parte real y parte imaginaria, del titanio en contacto con la solución de Ringer. Los diagramas de Nyquist y Bode muestran un comportamiento capacitivo, con un módulo de impedancia elevado y con dos constantes de tiempo. En la implementación de las integrales de KK se emplearon dos procedimientos, que se basan en un circuito equivalente que cumple las relaciones de KK y en una resistencia óhmica en paralelo añadida a los datos de impedancia medidos. Los resultados de impedancia del titanio satisfacen las relaciones de KK.

Palabras clave Titanio. Solución de Ringer. Relaciones de Kramers-Kronigs. Impedancia electroquímica.

1. INTRODUCTION

Electrochemical methods and electrochemical impedance spectroscopy (EIS) as analytical techniques, of low cost and easy to use, are frequently used in material characterisation, electrochemical, corrosion, microbiologically influenced corrosion (MIC) and biological applications[1-14].

At the present time there is increasing interest in the application of the frequency-domain integral relationships known as Kramers-Kronig (KK) relationships to analyse electrical measurements. KK relationships relate the real and imaginary parts of a measured impedance or the permittivity (ε) and conductivity (σ) of a material[15]. Two main uses have been devised for KK relationships: (I) to calculate the imaginary part of the impedance when only the real part is known, since the measurement of the real part is usually less prone to errors than the imaginary part; and (II) to assess the validity of a measured impedance when both the real and imaginary components are obtained experimentally. Some of the errors introduced by measuring will produce effects that can be identified by KK relationships, while other errors will not.

(•) Trabajo recibido el día 26 de julio de 2004 Y aceptado en su forma final el día 4 de octubre de 2004.
(*) School of Chemistry, University of St. Andrews, St. Andrews, Fife KY16 9ST, Scotland, United Kingdom.
(**) CENIM-National Centre for Metallurgical Research, CSIC, Avda. Gregorio del Amo 8, 28040 Madrid, Spain.
(***) School of Industrial Engineering, University of Castilla-La Mancha, Avda. Carlos III s/n, 45071 Toledo, Spain.

This paper studies the applicability of KK relationships to assess the validity of real and imaginary impedance measurements for titanium immersed in a Ringer's solution. Both the titanium material and the Ringer's solution were chosen as an example, and despite the fact that this system can be effectively characterised by standard chemical analytical tests, the methodologies to calculate KK integral relationships for impedance data are given, including a new proposal method based on an ohmic resistance shunted to the measured EIS data. The paper addresses the practical implementation of KK integral relationships when the available data covers only a finite frequency range. KK relationships allow it to be known if the acquisition of impedance data is correct and the data can be used to model the titanium/Ringer's solution system, or if there is an error in the acquisition procedure. The motivation of the study also included employing the EIS technique as a tool to investigate how the physical/chemical properties of titanium electrodes change with time in a Ringer's solution medium for up to 10 d.

2. MATERIAL AND METHODS

The tested titanium was of 99.2 wt.% purity (grade 2, ASTM F67-00 Standard) (UNS R50400). This material was chosen because it is used in ear piercing applications[16]. The chemical composition of the tested Ringer's solution was: 0.7195 g/100 ml NaCl, 0.2852 g/100 ml $MgSO_4$, 0.2623 g/100 ml Na_3PO_4, 0.0332 g/100 ml KCl.

The EIS method was used in the frequency range from 50×10^3 Hz to 3.15×10^{-3} Hz, allowing time for fast and slow processes to take place. A logarithmic sweeping frequency of 10 steps/decade was used. Impedance data was generated at the open circuit potential, i.e. without external polarisation, using immersion experiments. EIS involved the imposition of a small 10×10^{-3} V amplitude sine-wave. A Frequency Response Analyser (FRA), SOLARTRON model 1250, and an EG&G PARC potentiostat/galvanostat, model 273A, controlled by a computer, were used. All experiments were performed at 37 °C. The experimental procedure consisted of a conventional electrochemical glass cell, using a three-electrode cell arrangement with a platinum gauze (~36 cm^2 surface area) as counter electrode, a saturated calomel electrode (SCE) as reference electrode, and cold resin-mounted titanium as working electrode with 1 cm^2 surface area. The Ringer's solution was prepared using bidistilled water and tested immediately.

To study how the titanium/Ringer's solution system properties change with time, the experiments were performed (in triplicate) after 1, 3, 6 and 10 d of immersion. The EIS measurements were performed using three titanium specimens at each time point, under identical experimental conditions, in order to test their reproducibility, from high to low frequencies and from low to high frequencies.

2.1. Equivalent circuit model

The equivalent circuit of figure 1a was used to fit the impedance data for the titanium/Ringer's solution system, which contains two distributed constant phase elements (CPE_1 and CPE_2) to consider the two relaxation time constants (Fig. 2). R_S is the electrolyte resistance.

The admittance representation of the CPE (Y_{CPE}) shows a fractional-power dependent on the angular frequency (ω)

$$Y_{CPE} = Y_P \cdot (j\omega)^{\alpha} \qquad (1)$$

where Y_P is a real constant and $-1 < \alpha < 1$. When $\alpha = 0$, CPE is a resistor; when $\alpha = 1$, a capacitor; and when $\alpha = -1$, an inductor. Finally, if $\alpha = 0.5$, CPE is the Warburg admittance[17].

The calculated impedance ($Z_{cal}(\omega_i)$) of the equivalent circuit of figure 1a for a specific angular frequency value (ω_i) can be written as:

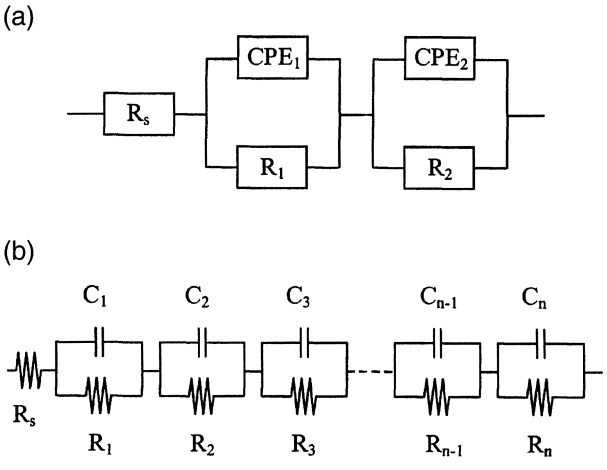

Figure 1. Equivalent circuits used to model the titanium/Ringer's solution system.

Figura 1. Circuitos equivalentes utilizados para modelar el sistema titanio/solución de Ringer.

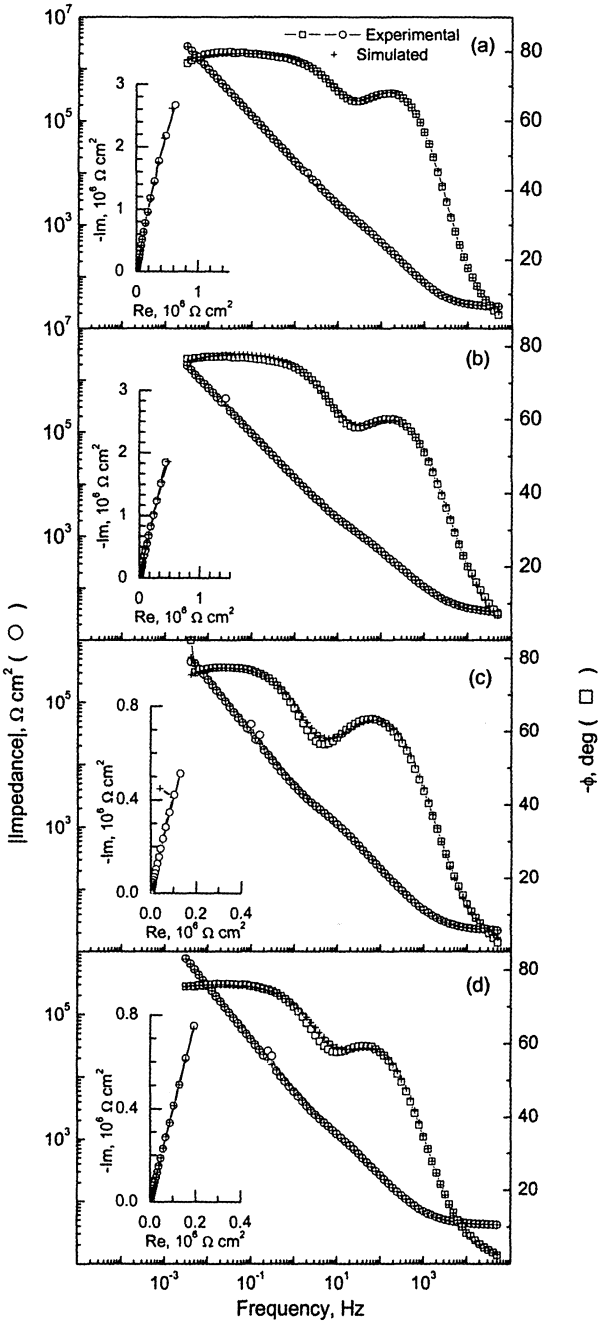

Figure 2. Bode plots for titanium after (a) 1, (b) 3, (c) 6 and (d) 10 d of immersion in a Ringer's solution.

Figura 2. Diagramas de Bode del titanio para (a) 1, (b) 3, (c) 6 y (d) 10 días de inmersión en la solución de Ringer.

$$Z_{cal}(\omega_i) = R_s + \frac{R_1}{1 + R_1 Y_{P1}(j\omega_i)^{\alpha 1}} + \frac{R_2}{1 + R_2 Y_{P2}(j\omega_i)^{\alpha 2}} \quad (2)$$

2.2. Kramers-Kronig (KK) integral relationships

KK relationships were applied in order to check the validity of the experimental impedance results. KK relationships are purely mathematical in nature, and hence do not reflect any particular physical condition[18]. KK relationships can be used as a diagnostic tool for the validation of a particular set of measured impedance data before fitting it to a mechanistic or electrical equivalent circuit model[19]. Thus, KK relationships are a suitable method to check if the experimental impedance data belongs to a linear and real electrical equivalent circuit or not. KK relationships can also be used to determine the real part (Re) (or the imaginary part, Im) of the impedance of a causal, stable, linear, time-invariant and finite system including $\omega \to 0$ and $\omega \to \infty$, when the change in the imaginary part (or the real part) with the angular frequency is known[20].

The integrals of KK relationships can be written as:

$$\mathrm{Re}Z(\omega) = \mathrm{Re}Z(\infty) + \left(\frac{2}{\pi}\right)\int_0^\infty \frac{x\,\mathrm{Im}Z(x) - \omega\,\mathrm{Im}Z(\omega)}{x^2 - \omega^2}dx \quad (3)$$

$$\mathrm{Im}Z(\omega) = \left(\frac{2\omega}{\pi}\right)\int_0^\infty \frac{\mathrm{Re}Z(x) - \mathrm{Re}Z(\omega)}{x^2 - \omega^2}dx \quad (4)$$

where $\mathrm{Re}Z(\omega)$ and $\mathrm{Im}Z(\omega)$ are the real and imaginary parts of the impedance, respectively; $0 < x < \infty$ (integration variable) and ω angular frequencies (rad s^{-1}). Using equation (3) it is possible to transform the imaginary part into the real part and vice versa, equation (4) [21-24].

It should be noted that equation (4) is frequently written with a minus sign $\left(\mathrm{Im}Z(\omega) = -\left(\frac{2\omega}{\pi}\right)\int_0^\infty \frac{\mathrm{Re}Z(x) - \mathrm{Re}Z(\omega)}{x^2 - \omega^2}dx\right)$ which reflects the convention to present complex impedance in (-Z"Z') coordinates, common in electrochemistry. This is, strictly speaking, erroneous, and may lead to confusion when equation (3) with minus sign in implemented in numerical procedures.

Comparison of the experimental plots with the plots calculated by the above method is a validation test for impedance measurements.

A complex non-linear least squares (CNLS) analysis was performed to fit the parameters of the equivalent circuit of figure 1a to the impedance data[25].

2.3. Average error ($\bar{E}$)

The consistency of the experimental impedance results was analysed by comparing the calculated

data with the experimental data, using an average percentage of error ($\bar{E}$). For instance, to compare the real part of the experimental impedance data with the real part of the impedance calculated using KK relationships, the $\bar{E}$ is given by:

$$\bar{E} = \frac{100}{N \times ReZ_{max}} \sum_{i=1}^{N} \left| ReZ_{exp}(\omega_i) - ReZ_{cal}(\omega_i) \right| \quad (5)$$

where ReZ_{max} is the maximum value of the real part of the experimental impedance data, and N is the number of points in the experimental data[20,26 and 27]. By writing Im instead of Re in equation (5), it is possible to compare the imaginary part of the experimental impedance data with the imaginary part of the impedance calculated using KK relationships and to evaluate the $\bar{E}$. As can be seen from equation (5), the $\bar{E}$ was normalised to the maximum value in the data set, in order to compare the different data sets, which may differ by orders of magnitude in their impedance values.

3. RESULTS AND DISCUSSION

Figure 2 shows typical Bode plots for the titanium specimens after 1, 3, 6 and 10 d of immersion in a Ringer's solution.

The fitted parameters of figure 2 are listed in table I, which also shows the estimated percentage of error for each parameter (in round brackets). As can be observed in figure 2, there is excellent agreement between the experimental results and the predictions of the model. Therefore, figure 1a is a good approach for modelling the titanium/Ringer's solution system.

When an equivalent circuit contains more elements than are represented by the data, a very large estimated error is obtained, indicating an incorrect model. While a large error confirms that the model is poor, a small error does not necessarily mean that the model is good, although this is one of the things that creates confidence in the model[28].

The Nyquist plots (inset of figure 2) show a capacitive behaviour with a high impedance modulus (11-68 × 10^6 Ω cm^2). Two capacitive loops are drawn in the Bode plots, defining two relaxation time constants characterised by two maxima in the ϕ axis.

The time constant (τ) for a CPE-R couple ($\tau = (RY_P)^{1/\alpha}$) is not single-valued, τ is distributed continuously or discretely around a mean value. The CPE_1-R_1 couple, which predominates at high frequencies, with a time constant within the order of magnitude of 10^{-2} s, may be originated by the titanium dioxide (TiO_2) film, frequently formed on titanium surfaces[29]. The CPE_2-R_2 couple, controlling at low frequencies, with a time constant within the order of magnitude of 10^3 s, characterises the properties of the TiO_2 film/Ringer's solution interface. Similar results have been reported in the literature[30]. Note that the smaller the τ, the faster the titanium/Ringer's solution system response.

The set of R_S, Y_{P1}, α_1, R_1, Y_{P2}, α_2 and R_2 parameters in table I were found by minimising the distances in the complex plane between a theoretical point and a measured point, as is shown in equation (6):

$$S = \sum_{i=1}^{N} \left\{ \left[\frac{ReZ_{exp}(\omega_i) - ReZ_{cal}(\omega_i)}{|Z_{exp}(\omega_i)|} \right]^2 + \left[\frac{ImZ_{exp}(\omega_i) - ImZ_{cal}(\omega_i)}{|Z_{exp}(\omega_i)|} \right]^2 \right\} \quad (6)$$

Table I. Parameters obtained from the fitting of impedance data for the titanium/Ringer's solution system

Tabla I. Parámetros obtenidos en el ajuste de los datos de impedancia del sistema titanio/solución de Ringer

Time d	R_S Ω cm^2	Y_{P1} μF cm^{-2} $s^{-(1-\alpha1)}$	α_1	R_1 Ω cm^2	Y_{P2} μF cm^{-2} $s^{-(1-\alpha2)}$	α_2	R_2 10^6 Ω cm^2
1	26 (0.4 %)	22.8 (3 %)	0.83 (0.5 %)	624 (3 %)	12.0 (0.2 %)	0.89 (0.1 %)	68 (7 %)
3	33 (0.3 %)	26.5 (1.8 %)	0.74 (0.3 %)	914 (1.7 %)	15.6 (0.2 %)	0.87 (0.1 %)	43 (6 %)
6	22 (0.3 %)	52.9 (1.1 %)	0.76 (0.2 %)	1078 (1.6 %)	46.7 (0.2 %)	0.87 (0.1 %)	11 (5 %)
10	41 (1.5 %)	56.8 (3.8 %)	0.75 (1.8 %)	652 (4.2 %)	36.2 (1 %)	0.85 (0.6 %)	55 (5 %)

Error is in brackets

where $ReZ_{exp}(\omega_i)$ and $ImZ_{exp}(\omega_i)$ are the real and imaginary parts of the measured impedance, respectively, for a specific angular frequency value (ω_i); and $ReZ_{cal}(\omega_i)$ and $ImZ_{cal}(\omega_i)$ are the real and imaginary parts of the calculated impedance, (equation 2), respectively, of the equivalent circuit of figure 1a) for a ω_i. Because the impedance spectrum covers a wide range of impedances, each data point was normalised by its magnitude $|Z_{exp}(\omega_i)|$ in order not to overemphasise data points with a large magnitude[31 and 32].

A Levenberg-Marquardt approach has been carried out to minimise S, (equation 6). The Levenberg-Marquardt method is a compromise between the Gauss-Newton method and the steepest descent method and is most useful when the parameter estimates are highly correlated, as is the case in the analysis of impedance data[33].

The α_2 values from table I are close to unity, indicating that the TiO_2 film suffers a deviation from the ideal capacitive behaviour ($\alpha_2 = 1$). This deviation has been attributed in the literature to rough and uneven surfaces[34]. The value of 0.85-0.89 for α_2 (table I) may indicate that the TiO_2 film formed on titanium specimens in a Ringer's solution is inhomogeneous. It may be a consequence of an intermediate oxidation phase, probably leading to local defects, flaws and even oxide roughness if the corresponding oxidised species dissolve into the Ringer's solution.

On the other hand, R_2 values of the order of 11-68 x 10^6 Ω cm^2 (table I) indicate the low corrosion of the passive film, corroborating the presence of a protective oxide on the titanium specimens. For 1, 3, 6 and 10 d of experimentation, a good fit between the experimental and calculated data was obtained.

Figure 3 shows the plots obtained using KK relationships from figure 2d, as an example. It can be observed that the experimental impedance data satisfies KK relationships, signifying stability for the titanium/Ringer's solution system. The stability of the EIS measurements over 10 d in the Ringer's solution was not affected, and the results are valid to be used to model the titanium/Ringer's solution system.

In the following paragraphs two different examples of procedures for checking KK relationships are discussed.

3.1. First example on the procedure of KK relationships

The first example consists of fitting the measured impedance data points to an equivalent circuit which satisfies KK relationships. If the measured data set can be fitted with such an equivalent circuit, then the experimental impedance data also satisfies KK relationships. As has been described above, the experimental impedance data in figure 2 can be simulated with the equivalent circuit in figure 1a. The parameter values for this circuit are indicated in table I. As the equivalent circuit in figure 1a satisfies KK relationships, the experimental data also satisfies KK relationships. It is concluded that figure 2 satisfies KK relationships.

For a more complicated experimental impedance spectrum than that of figure 2, a special equivalent circuit model may be used, consisting of a chain of series-connected parallel resistance-capacitor (R-C) circuits (Fig. 1b). The equivalent circuit in figure 1b satisfies KK relationships. Components R_i and C_i from the sub-circuit R_i-C_i may both simultaneously have negative values, indicating an inductive effect. If KK relationships, (equations 3 and 4), are directly used to check the

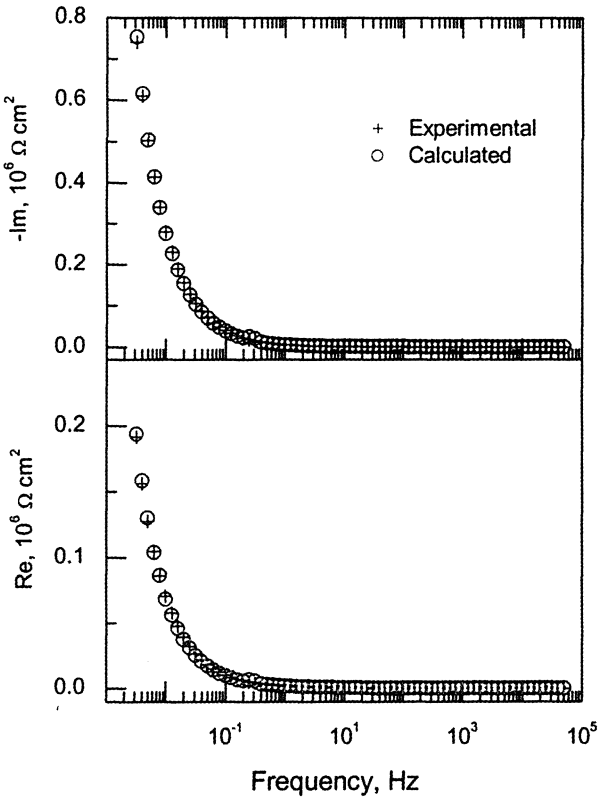

Figure 3. Comparison of experimental impedance data (+) and impedance calculated using KK relationships (o) for the titanium/Ringer solution system for 10 d.

Figura 3. Comparación de los datos experimentales de impedancia (+) y la impedancia calculada usando las relaciones de KK (o) del sistema titanio/solución de Ringer para 10 días de inmersión.

experimental impedance data, the integrals have to be evaluated from x = 0 to x = ∞, but, however, the impedance data is measured over a finite range of frequency (x_{low}, x_{high}). Thus it is necessary to extrapolate the impedance data below the lowest measured frequency, above the highest measured frequency, and between each successive pair of data (experimental and extrapolated data). For instance, to calculate the imaginary part (Im) of the impedance data from the measured real part (Re), equation (4) must be divided into three regions, the same would apply to equation (3):

$$\mathrm{Im}\,Z(\omega) = \left(\frac{2\omega}{\pi}\right)\left[\int_0^{x_{min}} \frac{\mathrm{Re}Z(x) - \mathrm{Re}Z(\omega)}{x^2 - \omega^2}dx + \right. \quad (7)$$

$$\left. + \int_{x_{min}}^{x_{max}} \frac{\mathrm{Re}Z(x) - \mathrm{Re}Z(\omega)}{x^2 - \omega^2}dx + \int_{x_{max}}^{\infty} \frac{\mathrm{Re}Z(x)\,\mathrm{Re}Z(\omega)}{x^2 - \omega^2}dx\right]$$

According to equation (7) it would only be necessary to extrapolate the experimental impedance data to lower (higher) frequencies up to a specific x value, x_{min} (x_{max}), ensuring that the contributions of the integrals from 0 to x_{min} and from x_{max} to ∞ (the tails) are negligible compared with the integral from x_{min} to x_{max}. This is achieved if x_{low}/x_{min} and x_{max}/x_{high} are typically between 100 and 1000 [18]. Therefore, from equation (7) it is possible to write:

$$\mathrm{Im}\,Z(\omega) \approx \left(\frac{2\omega}{\pi}\right)\int_{x_{min}}^{x_{max}} \frac{\mathrm{Re}Z(x) - \mathrm{Re}Z(\omega)}{x^2 - \omega^2}dx \quad (8)$$

Functions should be used for piece-wise interpolation of the experimental data for numerical integration. The integral in equation (8) can be evaluated in a piece-wise fashion by fitting a fifth-order polynomial coinciding with changes in the sign or gradient of ReZ(x) and ImZ(x) *vs.* frequency[23], or by fitting semilogarithmic polynomial expressions. The semilogarithmic form behaves well in the high-frequency regions where high-order polynomials exhibit oscillations[35]. These polynomials are used to generate a new set of data having properties that are desired for the numerical evaluation (see below). To avoid the singularity at x = ω, equation (8) can be split into two parts and the factor $\frac{1}{x^2 - \omega^2}$ expanded as a binomial series[26].

In this paper, to evaluate the integral of equation (8) from x_{min} to x_{max}, this is extended over each successive pair of data, where a natural cubic spline has been fitted[28].

Cubic splines have been obtained by considering ReZ(x) and -ImZ(x) *vs.* log(x) and using the following expression:

$$a[\log(x)]^3 + b[\log(x)]^2 + c[\log(x)] + d \quad (9)$$

By choosing log(x) instead of x as the independent variable, the data points appear equi-spaced in the frequency domain to carry out the fitting of cubic splines.

If a degree one polynomial is used between each successive pair of data, the resulting curve looks like a broken line. The fitting of a high degree polynomial to a set of data points is often unsatisfactory because the graph can wiggle to pass through the points. Nevertheless if the cubic polynomials are used, the first and the second derivatives can be made continuos, resulting in a smooth curve.

By extending the integral of equation (8) over each successive pair of data, some integrands exhibiting a singularity at the endpoints of the range of integration are obtained. To overcome this problem, a numerical integration method based on a Gauss-Legendre quadrature running in the MATLAB PROGRAM has been carried out[36]. Using this method it is not necessary to evaluate the integrand at the endpoints of the interval. The Gauss-Legendre quadrature technique approximates the integral of a particular function from the ordinates of the function at particular abscissas (at the zeros of the Gauss-Legendre polynomials) which are weighed and added together to give an approximate valuation of the integral[25]. The weights and the mesh on which the function is evaluated are chosen in such a way that the technique is exact for polynomials up to a given order.

3.2. Second example on the procedure of KK relationships

The second example on the applicability of KK relationships is also illustrated using the experimental data from figure 2d, in which the contribution of the integral from 5×10^4 Hz (the highest measured frequency) to x = ∞ is negligible, compared with the integral evaluated over the finite measured frequency range. Nevertheless, for

frequencies lower than 3.15 mHz it is necessary to extrapolate the impedance data below the lowest measured frequency (3.15 mHz). To avoid performing this extrapolation a method was proposed which generated a new impedance spectrum by considering a hypothetical selected ohmic resistance shunted (R_{shunt}) to the measured impedance data. In this way both the real (Re) and imaginary (Im) parts will have finite values from x = 0 to x = ∞.

If a R_{shunt} of 10^4 Ω cm^2 is chosen, the new generated impedance spectrum (Z_n) is calculated for each experimental frequency (ω_i) using the following expression:

$$Z_n(\omega_i) = \frac{Z_{exp}(\omega_i)R_{shunt}}{Z_{exp}(\omega_i) + R_{shunt}} \qquad (10)$$

and figure 4 shows the new generated Nyquist plot, from the impedance data of figure 2d and shunting a resistance of 10^4 Ω cm^2. The tails in figure 4 are negligible and the new generated impedance data can be directly checked through the KK relationships.

Figure 5 shows the comparison of the new generated experimental impedance of figure 4 and the impedance calculated using KK relationships. The new generated experimental impedance data satisfies KK relationships, and so the experimental impedance data (Fig. 2d) also satisfies KK relationships using this second procedure.

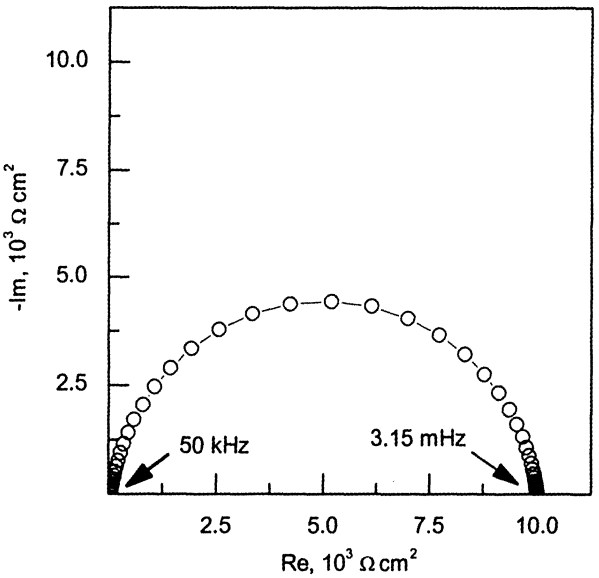

Figure 4. Nyquist plot for impedance data including an ohmic resistance shunted (R_{shunt}, 10^4 Ω cm^2) to the measured impedance data for 10 d immersion.

Figura 4. Diagrama de Nyquist del titanio para 10 días de inmersión, se ha incluido una resistencia en paralelo (R_{shunt}, 10^4 Ω cm^2) a los datos de impedancia.

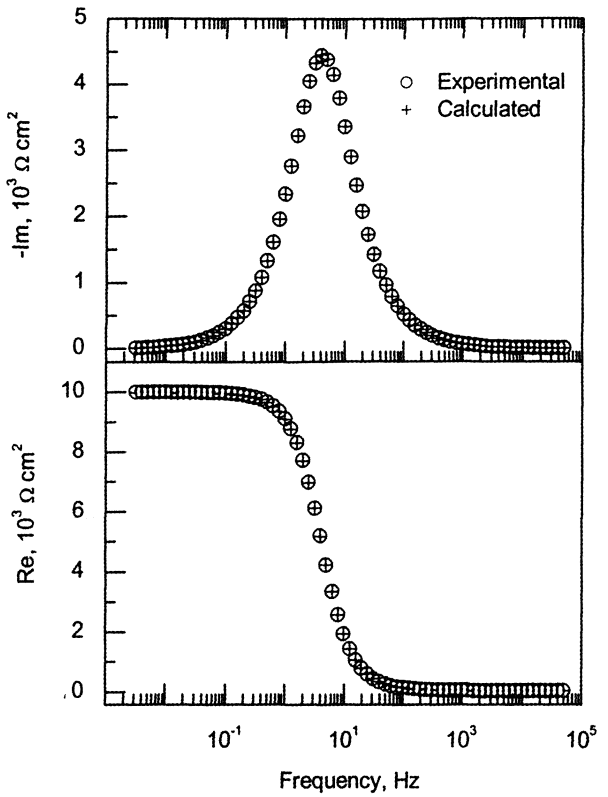

Figure 5. Comparison of experimental impedance data (+) and impedance calculated using KK relationships (o) for the titanium/Ringer's solution system for 10 d and an ohmic resistance shunted (R_{shunt}, 10^4 Ω cm^2).

Figura 5. Comparación de los datos experimentales de impedancia (+) y la impedancia calculada usando las relaciones de KK (o) del sistema titanio/solución de Ringer para 10 días de inmersión incluyendo una resistencia óhmica en paralelo (R_{shunt}, 10^4 Ω cm^2) a los datos de impedancia.

4. CONCLUSIONS

The shape of the Nyquist plots indicates a capacitive behaviour for the tested titanium showing two time constants, characterised by two maxima in the Bode plots (ϕ axis): at low frequencies originated by the TiO_2 film/Ringer's solution interface, and at high frequencies characterising the properties of the film (TiO_2) on the titanium. In general, the immersion of titanium in a Ringer's solution for up to 10 d does not affect the impedance properties.

The applicability of Kramers-Kronig (KK) relationships for validating impedance data for the titanium/Ringer's solution system has been assessed, finding that the experimental impedance

data satisfies KK relationships, indicating a stability process. This means that the experimental impedance data can be used to model the titanium/Ringer's solution system, and consequently the results are valid to be used in biological applications.

Acknowledgements

The authors express their gratitude to the Spanish Ministry of Science and Technology for financial support under Project MAT2001-1732-C02-01.

REFERENCES

[1] M.I. Sarrió, O. Alemán, D.A. Moreno, M. Roso y C. Ranninger, *Rev. Metal. Madrid* 40 (2004) 21-29.

[2] S.F. Medina, F.A. López y M. Morcillo, *Rev. Metal. Madrid* 39 (2003) 193-204.

[3] E. Bolaños-Rodríguez, S. Gil-Fundora, W. Francisco-Martín y J. Álvarez-Álvarez, *Rev. Metal. Madrid* 39 (2003) 210-214.

[4] J. Gregori, J. Agrisuelas, D. Giménez, M.P. Peña, J.J. García-Jareño y F. Vicente, *Rev. Metal. Madrid* 39 (2003) 346-356.

[5] N. Betancourt, F. Corvo, A. Mendoza, J. Simancas, M. Morcillo, J.A. González, F. Fragata, J.J. Peña, M. Sánchez de Villlaz, S. Flores, E. Almeida, S. Rivero y O.T. del Rincón, *Rev. Metal. Madrid*, Vol. Extr. (2003) 38-42.

[6] S.G. Gómez de Saravia, P.S. Guiamet y H.A. Videla, *Rev. Metal. Madrid*, Vol. Extr. (2003) 49-54.

[7] L. Espada, M. Sanjurjo, S. Urréjola, F. Bouzada, G. Rey y A. Sánchez, *Rev. Metal. Madrid*, Vol. Extr. (2003) 72-79.

[8] O. González y G. Santos, *Rev. Metal. Madrid*, Vol. Extr. (2003) 80-85.

[9] S.M. Traldi, J.L. Rosi e I. Costa, *Rev. Metal. Madrid*, Vol. Extr. (2003) 86-90.

[10] D.M. Escobar, C. Arroyave, F. Jaramillo, O.R. Mattos, I.C. Margarit y J. Calderón, *Rev. Metal. Madrid*, Vol. Extr. (2003) 97-103.

[11] J.A. González, M. Morcillo, E. Escudero, V. López, A. Bautista y E. Otero, *Rev. Metal. Madrid*, Vol. Extr. (2003) 110-115.

[12] A. Echavarría y C. Arroyave, *Rev. Metal. Madrid*, Vol. Extr. (2003) 174-181.

[13] L. Hernández, J.M. Miranda y O. Domínguez, *Rev. Metal. Madrid* 38 (2002) 108-116.

[14] C.M. Abreu, M.J. Cristóbal, P. Merino, X.R. Nóvoa, G. Pena y M.C. Pérez, *Rev. Metal. Madrid* 38 (2002) 315-325.

[15] P.J. Riu y C. Lapaz, *In Electrical Bioimpedance Methods: Applications to Medicine and Biotechnology*, P.J. Riu, J. Rosell, R. Bragós y O. Casas (Eds.), Annals of the Nueva York Academy of Science, Vol. 873, Nueva York, 1999, pp. 374-80.

[16] O.V. Correa, M. Saiki, S.O. Rogero e I. Costa, *Rev. Metal. Madrid*, Vol. Extr. (2003) 91-96.

[17] J.C. Wang, *J. Electrochem. Soc.* 134 (1987) 1915-1920.

[18] D.D. Macdonald, E. Sikora y G. Engelhardt, *Electrochim. Acta* 43 (1998) 87-107.

[19] G.S. Popkirov y R.N. Schindler, *Electrochim. Acta* 38 (1993) 861-872.

[20] J.M. Bastidas, J.L. Polo, C.L. Torres y E. Cano, *Corros. Sci.* 43 (2001) 269-281.

[21] P. Agarwal, M.E. Orazem y L.H. García-Rubio, *J. Electrochem. Soc.* 139 (1992) 1917-1927.

[22] C. Gabrielli, M. Keddam y H. Takenouti, *In Electrochemical Impedance: Analysis and Interpretation*, ASTM STP 1188, J.R. Scully, D.C. Silverman y M.W. Kendig (Eds.), Philadelphia, 1993, pp. 140-153.

[23] D.D. Macdonald y M. Urquidi-Macdonald, *J. Electrochem. Soc.* 132 (1985) 2316-2319.

[24] B.A. Boukamp, *J. Electrochem. Soc.* 142 (1995) 1885-1894.

[25] M. Abramowitz y A. Stegun, *Handbook of mathematical functions*, Dover Publications, Nueva York, 1964.

[26] M. Urquidi-Macdonald, S. Real y D.D. Macdonald, *J. Electrochem. Soc.* 133 (1986) 2018-2024.

[27] B.J. Dougherty y S.I. Smedly, *In Electrochemical Impedance: Analysis and Interpretation*, ASTM STP 1188, J.R. Scully, D.C. Silverman y M.W. Kendig (Eds.), Philadelphia, 1993, pp. 154-170.

[28] J.L. Polo, E. Cano y J.M. Bastidas, *J. Electroanal. Chem.* 537 (2002) 183-187.

[29] J.M. Bastidas, M. Saiki, S.O. Rogero, I. Costa y J.L. Polo, *J. Appl. Electrochem.* 32 (2002) 487-496.

[30] K. Azumi, T. Ohtsuka y N. Sato, *J. Electrochem. Soc.* 134 (1987) 1352-1357.

[31] J.R. Macdonald, J. Schoonman y A.P. Lehnen, *J. Electroanal. Chem.* 131 (1982) 77-95.

[32] G. Spinolo, G. Chiodelli, A. Magistris y U.A. Tamburini, *J. Electrochem. Soc.* 135 (1988) 1419-1424.

[33] R.L. Zeller III y R.F. Savinell, *Corros. Sci.* 26 (1986) 591-599.

[34] U. Rammelt y G. Reinhard, *Electrochim. Acta* 35 (1990) 1045-1049.

[35] M.E. Orazem, J.M. Esteban y O.C. Moghissi, *Corrosion* 47 (1991) 248-259.

[36] G.J. Borse, *Numerical Methods with MATLAB*, PWS Publishing Company, Boston, Massachusetts, 1997, p. 181.